Human Molecular Genetics, 2011, Vol. 20, No. 3 **445–454**
doi:10.1093/hmg/ddq491
Advance Access published on November 9, 2010

Tsc2 gene inactivation causes a more severe epilepsy phenotype than *Tsc1* inactivation in a mouse model of Tuberous Sclerosis Complex

Ling-Hui Zeng[1,2,3], Nicholas R. Rensing[2,3], Bo Zhang[2,3], David H. Gutmann[2], Michael J. Gambello[4] and Michael Wong[2,3,*]

[1]Department of Pharmacy, Zhejiang University City College, Hangzhou, Zhejiang 310015, China, [2]Department of Neurology and [3]Hope Center for Neurological Disorders, Washington University School of Medicine, St Louis, MO 63110, USA and [4]Division of Medical Genetics, Department of Pediatrics, University of Texas Health Science Center, 6431 Fannin Street, MSB 3.144, Houston, TX 77030, USA

Received April 2, 2010; Revised and Accepted November 4, 2010

Tuberous Sclerosis Complex (TSC) is an autosomal dominant, multi-system disorder, typically involving severe neurological symptoms, such as epilepsy, cognitive deficits and autism. Two genes, *TSC1* and *TSC2*, encoding the proteins hamartin and tuberin, respectively, have been identified as causing TSC. Although there is a substantial overlap in the clinical phenotype produced by *TSC1* and *TSC2* mutations, accumulating evidence indicates that *TSC2* mutations cause more severe neurological manifestations than *TSC1* mutations. In this study, the neurological phenotype of a novel mouse model involving conditional inactivation of the *Tsc2* gene in glial-fibrillary acidic protein (GFAP)-positive cells (*Tsc2*^{GFAP1}CKO mice) was characterized and compared with previously generated *Tsc1*^{GFAP1}CKO mice. Similar to *Tsc1*^{GFAP1}CKO mice, *Tsc2*^{GFAP1}CKO mice exhibited epilepsy, premature death, progressive megencephaly, diffuse glial proliferation, dispersion of hippocampal pyramidal cells and decreased astrocyte glutamate transporter expression. However, *Tsc2*^{GFAP1}CKO mice had an earlier onset and higher frequency of seizures, as well as significantly more severe histological abnormalities, compared with *Tsc1*^{GFAP1}CKO mice. The differences between *Tsc1*^{GFAP1}CKO and *Tsc2*^{GFAP1}CKO mice were correlated with higher levels of mammalian target of rapamycin (mTOR) activation in *Tsc2*^{GFAP1}CKO mice and were reversed by the mTOR inhibitor, rapamycin. These findings provide novel evidence in mouse models that *Tsc2* mutations intrinsically cause a more severe neurological phenotype than *Tsc1* mutations and suggest that the difference in phenotype may be related to the degree to which *Tsc1* and *Tsc2* inactivation causes abnormal mTOR activation.

INTRODUCTION

Tuberous Sclerosis Complex (TSC) is an autosomal dominant genetic disorder, resulting from the mutation of either the *TSC1* or *TSC2* genes and involving tumor or hamartoma formation in multiple organs (1–3). Neurological involvement, including epilepsy, cognitive deficits and autism, often constitutes the most disabling symptoms of the disease. Although there is a substantial overlap in the clinical phenotype of TSC produced by *TSC1* and *TSC2* mutations, accumulating evidence indicates that *TSC2* mutations cause more severe neurological manifestations than *TSC1* mutations (4–7). In particular, patients with TSC2 mutations tend to have an earlier onset and higher frequency of seizures, as well as more severe cognitive deficits.

The mechanistic basis for these differences in phenotype–genotype correlation is unknown, but may involve differences in the ability of the *TSC1* and *TSC2* gene products, hamartin and tuberin, to regulate the mammalian target of rapamycin (mTOR) pathway. Hamartin and tuberin bind together to form a single functional complex (8–10), which collectively exerts its downstream effects and likely explains the

*To whom correspondence should be addressed at: Department of Neurology, Washington University School of Medicine, 660 South Euclid Avenue, Box 8111, St Louis, MO 63110, USA. Tel: +1 3143628713; Fax: +1 3143629462; Email: wong_m@wustl.edu

overlapping phenotypes resulting from both *TSC1* and *TSC2* mutations. The hamartin–tuberin complex acts as a GTPase-activating protein (GAP) to inhibit the mTOR pathway by first inactivating the small GTPase protein, Rheb (Ras homolog expressed in brain) (11–16). As mTOR controls a variety of downstream functions involved in protein synthesis, cell growth, proliferation, metabolism and synaptic plasticity, hyperactivation of the mTOR pathway due to *TSC* gene mutations likely accounts for many of the phenotypic features of TSC. Since tuberin, but not hamartin, contains the GAP-related domain (17), *TSC2* mutations may have more disruptive effects than *TSC1* mutations on the GAP activity of the hamartin–tuberin complex, and thus may cause greater dysregulation of the mTOR pathway and more severe phenotypic effects.

The neurological phenotype of a mouse model of TSC due to conditional inactivation of the *Tsc1* gene in glial-fibrillary acidic protein (GFAP)-positive cells ($Tsc1^{GFAP1}$CKO mice) has previously been extensively characterized. These $Tsc1^{GFAP1}$CKO mice exhibit spontaneous epilepsy and premature death related to progressive glial proliferation, impaired glial buffering mechanisms and hippocampal neuronal disorganization (18–25). The development of this neurological phenotype of $Tsc1^{GFAP1}$CKO mice is almost completely prevented by early treatment with the mTOR inhibitor, rapamycin, indicating that mTOR hyperactivation is primarily responsible for causing these phenotypic features (26). More recently, a conditional knock-out (KO) mouse model involving *Tsc2* gene inactivation was generated (27), driven by a different GFAP transgenic line from that used in $Tsc1^{GFAP1}$CKO mice (28). While these $Tsc2^{GFAP2}$CKO [designated $Tsc2^{GFAP2}$CKO to distinguish the different Cre-recombinase (Cre) drivers] mice exhibit many overlapping features with the $Tsc1^{GFAP1}$CKO mice, a direct comparison cannot be made due to the different cellular expression of Cre. Thus, in this study, we have generated a new $Tsc2^{GFAP1}$CKO mouse line, using the same GFAP-Cre line used to generate the $Tsc1^{GFAP1}$CKO mice (18,29) and allowing a more direct comparison of the effects of *Tsc1* versus *Tsc2* inactivation. To our knowledge, this is the first study to directly compare the phenotypic effects of *Tsc1* and *Tsc2* inactivation in mouse models of neurological disease.

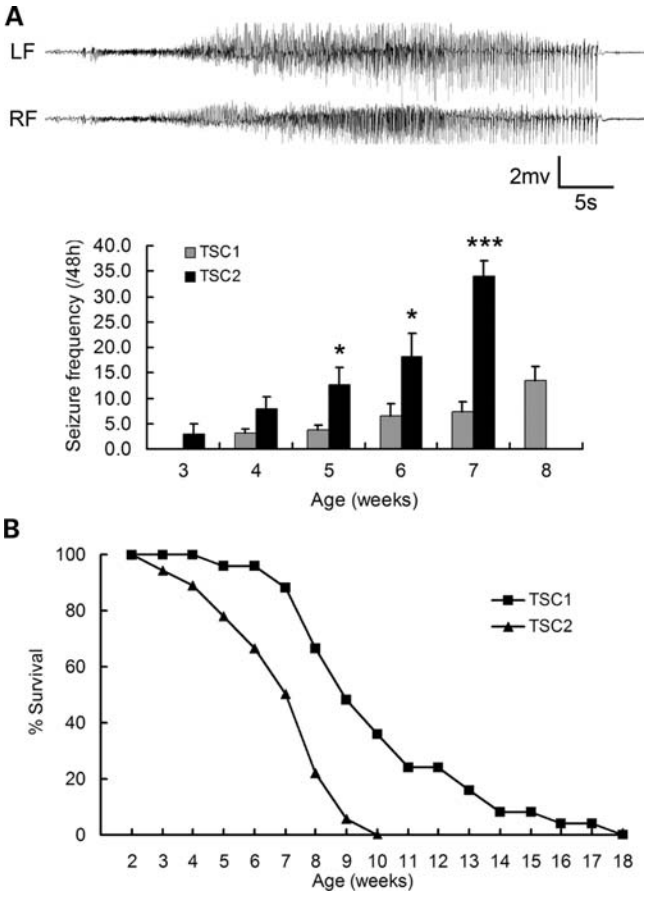

Figure 1. $Tsc2^{GFAP1}$CKO mice have more severe epilepsy and earlier premature death than $Tsc1^{GFAP1}$CKO mice. (**A**) $Tsc1^{GFAP1}$CKO and $Tsc2^{GFAP1}$CKO mice underwent video-EEG monitoring starting at 3 weeks of age. The EEG tracings show a typical electrographic seizure from a $Tsc2^{GFAP1}$CKO mice, typically characterized behaviorally by head nodding, rearing, and repetitive forelimb clonus. LFand RF, left and right frontal epidural electrodes. Seizures occur in $Tsc2^{GFAP1}$CKO mice at 3 weeks and become progressively more frequent with age. Note that no $Tsc2^{GFAP1}$CKO mice survived long enough in the video-EEG studies to collect seizure frequency data at 8 weeks. In contrast, in $Tsc1^{GFAP1}$CKO mice, seizures do not start until at least 4 weeks of life and the seizure frequency is significantly lower than in $Tsc2^{GFAP1}$CKO mice ($^{*}P < 0.05$, $^{***}P < 0.001$ by ANOVA, $n = 16$ for $Tsc2^{GFAP1}$CKO and $n = 22$ for $Tsc1^{GFAP1}$CKO mice). (**B**) Both $Tsc1^{GFAP1}$CKO and $Tsc2^{GFAP1}$CKO mice exhibit premature death, but $Tsc2^{GFAP1}$CKO die earlier than $Tsc1^{GFAP1}$CKO mice ($P < 0.05$ by the Kaplan–Meier log-rank test, $n = 18$ for $Tsc2^{GFAP1}$CKO and $n = 25$ for $Tsc1^{GFAP1}$CKO mice).

RESULTS

$Tsc2^{GFAP1}$CKO mice have more severe epilepsy and earlier premature death than $Tsc1^{GFAP1}$CKO mice

$Tsc2^{GFAP1}$CKO mice appear grossly normal for the first couple weeks of life, but at around 2–3 weeks of life, they begin to have observable seizures, characterized primarily by head nodding, rearing up on the hindlimbs, repetitive forelimb clonus and occasional loss of upright posture with generalized repetitive clonus of all limbs. Video-electroencephalography (EEG) recordings confirm that $Tsc2^{GFAP1}$CKO mice have occasional (3.0 ± 2.0/48 h) seizures at 3 weeks of age, which become progressively more frequent over the ensuing month (Fig. 1A). In contrast, $Tsc1^{GFAP1}$CKO mice have no seizures at 3 weeks and have significantly fewer seizures in subsequent weeks than $Tsc2^{GFAP1}$CKO mice. $Tsc2^{GFAP1}$CKO mice subsequently experience poor weight gain (Supplementary Material, Fig. S1) and premature death with 50% mortality around 7 weeks of age and 100% mortality by 10 weeks (Fig. 1B). $Tsc1^{GFAP1}$CKO mice also exhibit poor weight gain and premature death, but live significantly longer than $Tsc2^{GFAP1}$CKO mice. The causes of death in both $Tsc1^{GFAP1}$CKO and $Tsc2^{GFAP1}$CKO mice were similar, related to either acute seizures/status epilepticus or malnutrition/dehydration.

Since both $Tsc1^{GFAP1}$CKO and $Tsc2^{GFAP1}$CKO mice were bred on a mixed genetic background primarily involving SV129 mouse strain (SV129) and C57 black 6 mouse strain (C57Bl6) parental strains, we performed SNP genotyping to determine whether the phenotypic differences might relate to different genetic contributions of the parental strains. In an

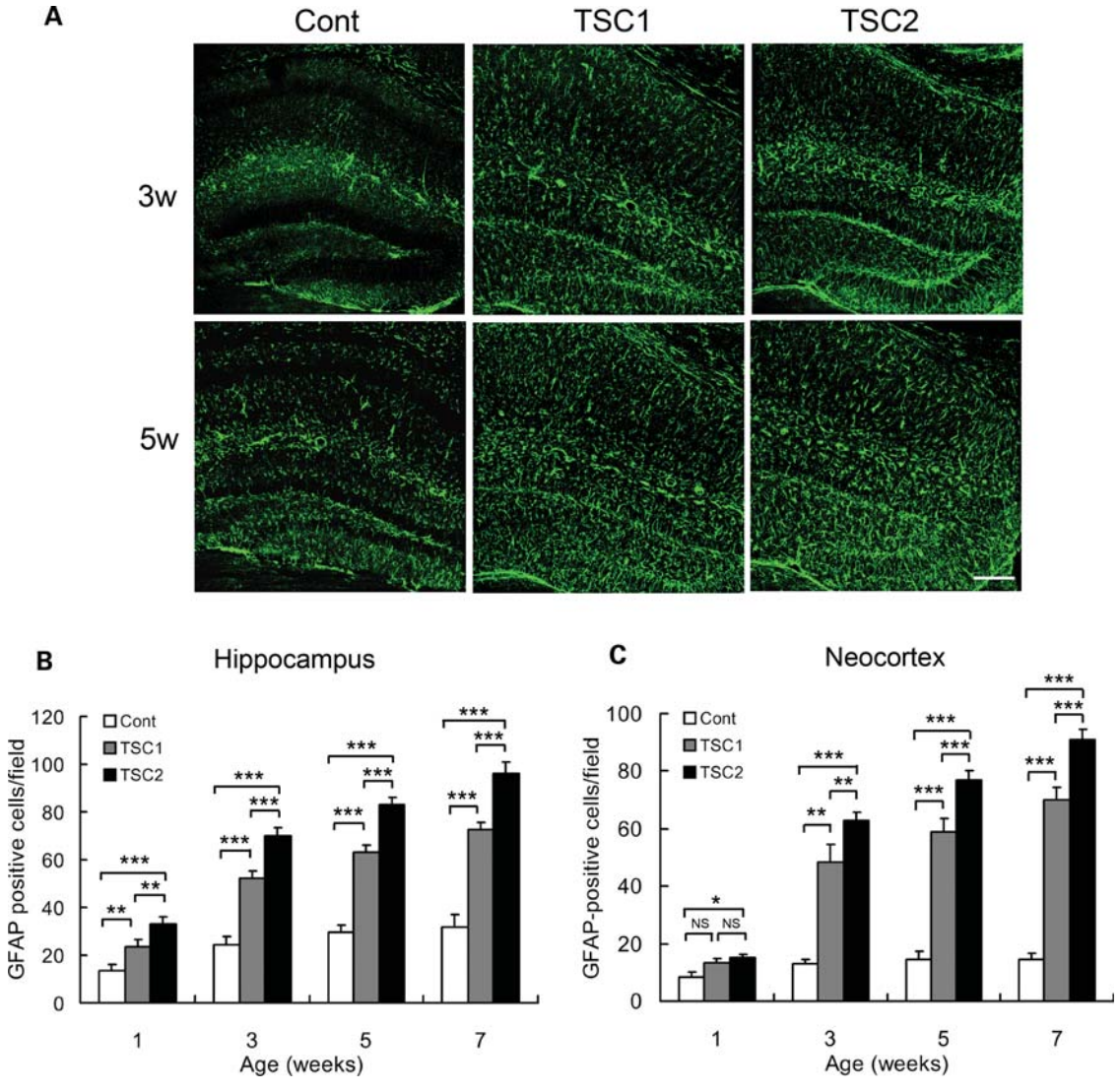

Figure 2. *Tsc2*^{GFAP1}CKO mice have more severe astrocyte proliferation than *Tsc1*^{GFAP1}CKO mice. (**A**) GFAP-staining was performed in control, *Tsc1*^{GFAP1}CKO and *Tsc2*^{GFAP1}CKO mice at different ages. Both *Tsc1*^{GFAP1}CKO and *Tsc2*^{GFAP1}CKO mice exhibited a significant increase in GFAP-positive cells in hippocampus compared with control mice. Scale bar = 200 μm. (**B** and **C**) Quantitative analysis of both hippocampus and neocortex shows that the increase in GFAP-positive cells is significantly greater in *Tsc2*^{GFAP1}CKO mice compared with *Tsc2*^{GFAP1}CKO mice ($^{*}P < 0.05$, $^{**}P < 0.01$, $^{***}P < 0.001$ by ANOVA, $n = 6$ mice per group).

analysis of 231 SNPs that differentiated between SV129 and C57Bl6 genetic strains, the relative contribution of these strains was very similar in *Tsc1*^{GFAP1}CKO and *Tsc2*^{GFAP1}CKO mice ($77 \pm 3\%$ SV129 in *Tsc1*^{GFAP1}CKO versus $76 \pm 3\%$ SV129 in *Tsc2*^{GFAP1}CKO mice, $P = 0.62$, $n = 5$ per group).

Tsc2^{GFAP1}CKO mice have more severe astrocyte proliferation, neuronal disorganization and megencephaly than Tsc1^{GFAP1}CKO mice

Histologically, *Tsc2*^{GFAP1}CKO mice develop a progressive increase in astrocyte number diffusely throughout the brain, but most obviously in neocortex and hippocampus (Fig. 2). This astrocyte proliferation is detectable as early as 1 week of life, becomes progressively more severe beyond 3 weeks of age and is at least partially due to regional cell proliferation in dentate gyrus and cortex (Supplementary Material, Fig. S2). By comparison, *Tsc1*^{GFAP1}CKO mice also exhibit similar increases in astrocytes, but the onset is slightly later and severity is significantly less than in *Tsc2*^{GFAP1}CKO mice (~1.3-fold increase in GFAP-positive cells in neocortex and hippocampus of *Tsc2*^{GFAP1}CKO compared with *Tsc1*^{GFAP1}CKO mice; Fig. 2). There is also a progressive neuronal disorganization in *Tsc2*^{GFAP1}CKO mice, most apparent in hippocampus with a dispersion of the pyramidal cell layer (Fig. 3A), which is similar to, but more severe than, *Tsc1*^{GFAP1}CKO mice. CA1 pyramidal cell layer width was significantly greater in *Tsc2*^{GFAP1}CKO mice than *Tsc1*^{GFAP1}CKO mice and controls [141.2 ± 4.8 vs. 110.7 ± 2.6 and 77.6 ± 1.6 μm, respectively, at 3 weeks of age; $P < 0.01$ by analysis of variance (ANOVA) between all three groups, $n = 6$ mice per group]. By comparison, the laminar organization and neuronal structure in neocortex was grossly intact. These glial and

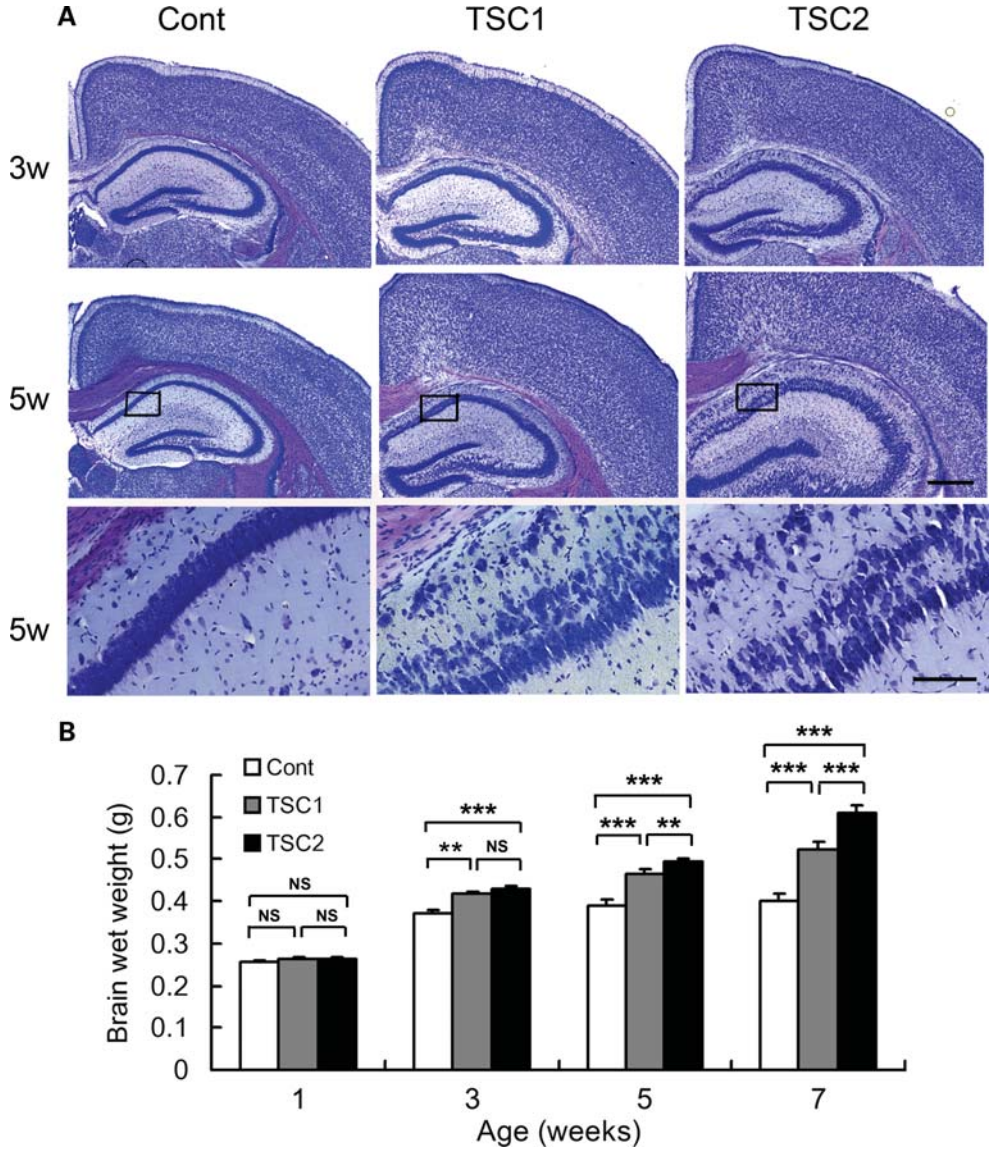

Figure 3. *Tsc2*^{GFAP1}CKO mice have more severe neuronal disorganization and megencephaly than *Tsc1*^{GFAP1}CKO mice. (**A**) Cresyl violet staining demonstrated an obvious dispersion of the pyramidal cell layer in hippocampus of both *Tsc1*^{GFAP1}CKO and *Tsc2*^{GFAP1}CKO compared with controls, but this was more pronounced in *Tsc2*^{GFAP1}CKO mice. Scale bars = 200 μm and 100 μm for low- and high-power images, respectively. (**B**) Brain weight was significantly increased in both *Tsc1*^{GFAP1}CKO and *Tsc2*^{GFAP1}CKO mice compared with controls starting at 3 weeks of age, and was greater in *Tsc2*^{GFAP1}CKO mice compared with *Tsc1*^{GFAP1}CKO mice starting at 5 weeks of age ($^{**}P < 0.01$, $^{***}P < 0.001$ by ANOVA, $n = 6$ mice per group).

neuronal histological abnormalities in neocortex and hippocampus contribute to a gross, generalized megencephaly and increased brain weight in *Tsc2*^{GFAP1}CKO mice starting at 3 weeks of age and becoming progressively more obvious with time (Fig. 3B). The increased brain size and weight in *Tsc2*^{GFAP1}CKO mice are significantly more (~1.2-fold more at 7 weeks of age) than in *Tsc1*^{GFAP1}CKO mice.

The more severe neurological phenotype of Tsc2^{GFAP1}CKO mice is associated with greater mTOR hyperactivation than Tsc1^{GFAP1}CKO mice and can be reversed by rapamycin

The histological abnormalities and epilepsy in *Tsc1*^{GFAP1}CKO mice have previously been shown to be directly related to hyperactivation of the mTOR pathway, as the mTOR inhibitor rapamycin can almost completely prevent these abnormalities (26). Similarly, *Tsc2*^{GFAP1}CKO mice exhibit increased mTOR activation compared with control mice, as reflected by increased phospho-S6 (P-S6) expression (Fig. 4A). In addition, expression of the astrocyte glutamate transporter GLT-1 is decreased in *Tsc2*^{GFAP1}CKO mice compared with controls (Fig. 4B). When directly comparing mTOR activation between *Tsc1*^{GFAP1}CKO and *Tsc2*^{GFAP1}CKO mice, P-S6 expression was significantly greater in *Tsc2*^{GFAP1}CKO mice (1.45 ± 0.16-fold more than *Tsc1*^{GFAP1}CKO mice at 3 weeks of age, $P < 0.05$ by *t*-test, $n = 6$ mice per group), but there was no significant difference in the decreased GLT-1 comparing *Tsc1*^{GFAP1}CKO and *Tsc2*^{GFAP1}CKO mice (Fig. 4C). In addition, while hamartin expression is decreased in the brains

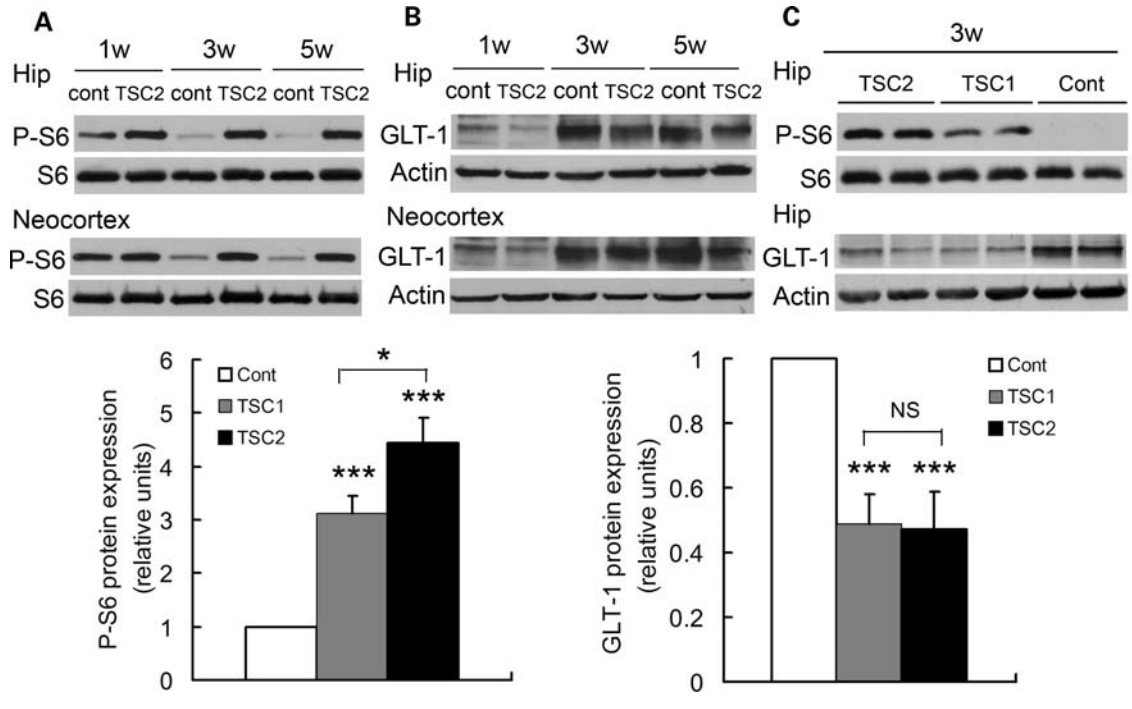

Figure 4. *Tsc2*^{GFAP1}CKO mice have greater mTOR hyperactivation than *Tsc1*^{GFAP1}CKO mice. (**A**) Total S6 and phospho-S6 (P-S6) expression was measured by Western blotting in neocortex and hippocampus of control and *Tsc2*^{GFAP1}CKO mice. mTOR activation, as reflected by P-S6 expression, is increased in *Tsc2*^{GFAP1}CKO mice compared with controls. (**B**) *Tsc2*^{GFAP1}CKO mice also have decreased GLT-1 expression compared with controls. (**C**) Although there is no difference in GLT-1 expression between *Tsc1*^{GFAP1}CKO and *Tsc2*^{GFAP1}CKO mice, mTOR activation is significantly greater in *Tsc2*^{GFAP1}CKO mice compared with control mice Representative blots are shown. Graphs show summarized quantified data for all experiments ($^{*}P < 0.05$, $^{***}P < 0.001$ by ANOVA, each experiment was repeated three times with $n = 6$ mice total per group).

of *Tsc1*^{GFAP1}CKO mice and tuberin expression is decreased in *Tsc2*^{GFAP1}CKO mice as would be expected from the genes targeted, there are no definite corresponding changes in the other protein (i.e. tuberin in *Tsc1*^{GFAP1}CKO mice and hamartin in *Tsc2*^{GFAP1}CKO mice; Supplementary Material, Fig. S3). Overall, these results suggest that *Tsc2* inactivation causes greater mTOR pathway activation compared with *Tsc1* inactivation, and that the larger mTOR hyperactivation in *Tsc2*^{GFAP1}CKO mice likely reflects a direct effect on tuberin.

To determine whether mTOR hyperactivation mediates the histological and behavioral phenotype of *Tsc2*^{GFAP1}CKO mice, we initiated rapamycin treatment at 2 weeks of age. Rapamycin inhibited the increased P-S6 expression of *Tsc2*^{GFAP1}CKO mice (Fig. 5A). Rapamycin also decreased the megencephaly and number (Fig. 5B) and proliferation (Supplementary Material, Fig. S2) of astrocytes in *Tsc2*^{GFAP1}CKO mice, and reduced the dispersion of the pyramidal cell layer in hippocampus (Fig. 5C). Finally, rapamycin-treated *Tsc2*^{GFAP1}CKO mice exhibited significantly fewer seizures (Fig. 5D), improved weight gain (Supplementary Material, Fig. S1) and prolonged survival (Fig. 5E), compared with vehicle-treated *Tsc2*^{GFAP1}CKO mice. These effects of rapamycin in *Tsc2*^{GFAP1}CKO mice were very similar to those seen in *Tsc1*^{GFAP1}CKO mice (26), suggesting that the mTOR activation mediates the neurological phenotype of both *Tsc2*^{GFAP1}CKO and *Tsc1*^{GFAP1}CKO mice and that the differences in the degree of mTOR activation (Fig. 4) may account for the differences in severity of the phenotype of *Tsc1*^{GFAP1}CKO and *Tsc2*^{GFAP1}CKO mice.

DISCUSSION

TSC represents one of the most common single-gene disorders causing epilepsy and results from mutations of either the *TSC1* or *TSC2* gene. Although there is substantial overlap and similarities in the phenotype of TSC due to *TSC1* and *TSC2* mutations, a number of studies indicate that *TSC2* mutations produce more severe phenotypic features, including the severity and frequency of epilepsy and other neurological symptoms (4–7). The underlying mechanisms responsible for any phenotypic variability between *TSC1* and *TSC2* mutations are poorly understood, but have been hypothesized to relate to differential effects of *TSC1* and *TSC2* mutations on Rheb-mTOR pathway regulation by the hamartin–tuberin complex. In this study, we have generated a novel *Tsc2*^{GFAP1}CKO mouse model and directly compared its phenotype to *Tsc1*^{GFAP1}CKO mice to assess differences in the effects of *Tsc1* and *Tsc2* gene inactivation on epilepsy and associated histological and molecular brain abnormalities. While *Tsc2*^{GFAP1}CKO mice have qualitatively similar features as *Tsc1*^{GFAP1}CKO mice, the neurological phenotype was more severe in *Tsc2*^{GFAP1}CKO mice. Furthermore, these phenotypic differences could likely be attributed to differences in the degree of mTOR hyperactivation. To our knowledge, this is the first study directly comparing the effects of *Tsc1* and *Tsc2* gene inactivation in mouse models of neurological disease.

The findings from this study indicate that there are intrinsic differences in the effects of *Tsc1* and *Tsc2* gene inactivation on

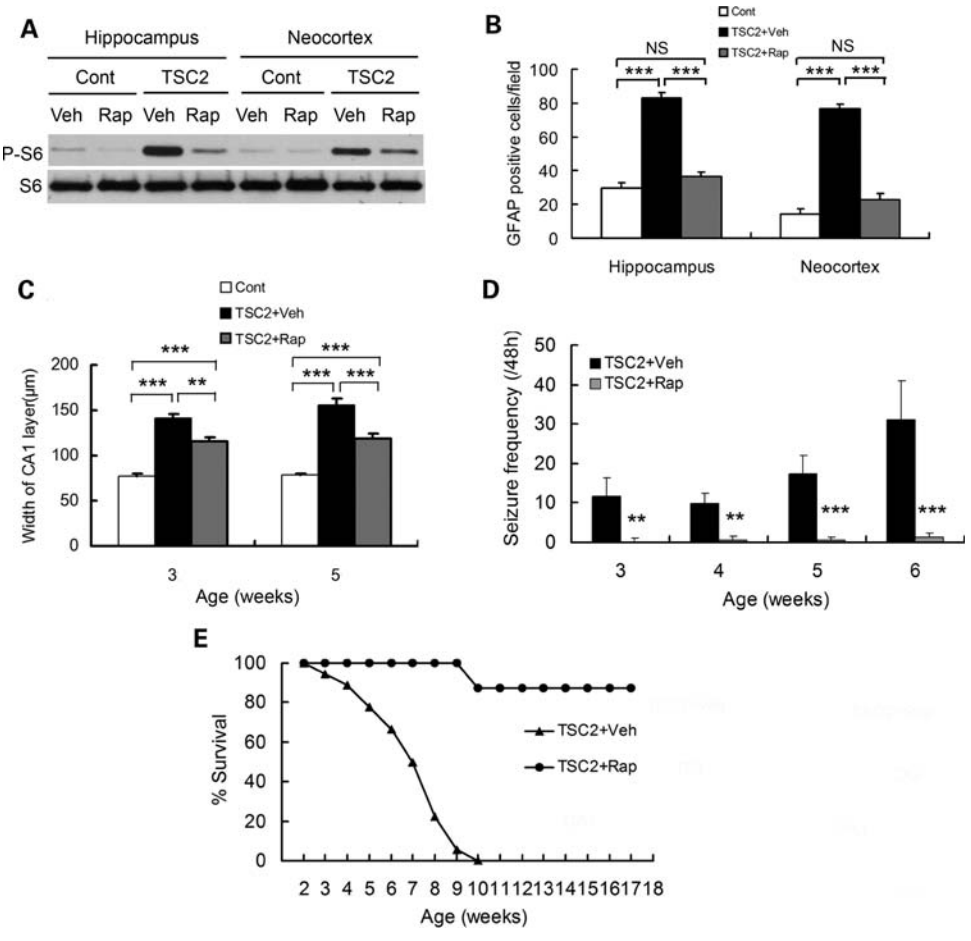

Figure 5. The neurological phenotype of *Tsc2*^{GFAP1}CKO mice is prevented by rapamycin. (**A**) Rapamycin inhibits mTOR activation, as reflected by P-S6 expression by Western blotting, in *Tsc2*^{GFAP1}CKO mice. (**B**) Rapamycin prevents the increase in GFAP-positive cells in *Tsc2*^{GFAP1}CKO mice (***$P <$ 0.001 by ANOVA, $n = 6$ mice per group). (**C**) Rapamycin decreases, but does not completely prevent, the dispersion of the pyramidal cell layer in hippocampus (**$P < 0.01$, ***$P < 0.001$ by ANOVA, $n = 6$ mice per group). (**D**) Rapamycin decreases seizure frequency in *Tsc2*^{GFAP1}CKO mice (**$P < 0.01$, ***$P < 0.001$ by ANOVA, $n = 18$ for *Tsc2*^{GFAP1}CKO and $n = 8$ for *Tsc2*^{GFAP1}CKO + Rap groups). (**E**) Rapamycin also prolongs survival of *Tsc2*^{GFAP1}CKO mice ($P < 0.05$ by the Kaplan–Meier log-rank test, $n = 19$ for *Tsc2*^{GFAP1}CKO and $n = 8$ for *Tsc2*^{GFAP1}CKO + Rap groups).

neurological manifestations of TSC. *Tsc2*^{GFAP1}CKO had an earlier onset of epilepsy, a higher seizure frequency and earlier mortality compared with *Tsc1*^{GFAP1}CKO mice. The differences in the epilepsy phenotype between *Tsc1*^{GFAP1}CKO and *Tsc2*^{GFAP1}CKO mice were associated with corresponding differences in the underlying pathological processes that likely promote epileptogenesis in these mice. In particular, the degree of glial proliferation, neuronal disorganization and resulting megencephaly was greater in *Tsc2*^{GFAP1}CKO mice. In contrast, there was no significant difference in GLT-1 expression between *Tsc1*^{GFAP1}CKO and *Tsc2*^{GFAP1}CKO mice. Thus, while the relative contribution of these different pathological and molecular abnormalities to epileptogenesis in both mouse models is not specifically known, these results suggest that these mechanisms may be differentially regulated by *Tsc1* versus *Tsc2* inactivation. In any case, qualitatively *Tsc1*^{GFAP1}CKO and *Tsc2*^{GFAP1}CKO mice exhibited similar neurological features and the differences between these mice primarily consisted of quantitative differences in the various abnormalities, such as earlier age of onset of epilepsy and associated pathological markers. As hyperactivation of the mTOR pathway is the likely pathophysiological trigger for a number of the manifestations of TSC, the observed difference in mTOR activation/P-S6 expression between *Tsc1*^{GFAP1}CKO and *Tsc2*^{GFAP1}CKO mice may account for the differences in phenotypic severity in these mice. Furthermore, the ability of rapamycin to almost completely prevent the phenotypical features of *Tsc2*^{GFAP1}CKO mice indicates that abnormal mTOR signaling is critically involved in the neurological phenotype of these mice. As similar effects of rapamycin are observed in *Tsc1*^{GFAP1}CKO mice (26), this also provides evidence that differences in mTOR activation account for the phenotypic differences between *Tsc1*^{GFAP1}CKO and *Tsc2*^{GFAP1}CKO mice. Thus, the increased mTOR activation in *Tsc2*^{GFAP1}CKO mice likely causes greater amplification of downstream epileptogenic mechanisms compared with *Tsc1*^{GFAP1}CKO mice.

The molecular mechanisms accounting for this difference in the effects of *TSC1* and *TSC2* inactivation on mTOR activation are unknown, but may relate to the interaction of the hamartin–tuberin complex with the small GTPase protein, Rheb. The hamartin–tuberin complex acts as a GAP to

inhibit the mTOR pathway by first inactivating Rheb. Since tuberin, but not hamartin, contains the GAP-related domain (17), *TSC2* mutations may have more disruptive effects than *TSC1* mutations on the GAP activity of the hamartin–tuberin complex, and thus may cause greater dysregulation of the mTOR pathway. For example, total loss of tuberin from a TSC2 mutation would completely eliminate GAP activity of the hamartin–tuberin complex, whereas hamartin loss may just destabilize the hamartin–tuberin complex, making tuberin GAP function less efficient. Alternatively, *TSC2* and *TSC1* mutations could have differential effects on the stability of hamartin or tuberin in the absence of the deficient protein. The lack of obvious decrease in hamartin expression in *Tsc2*^{GFAP1}CKO mice and vice versa suggests that the larger effect of *Tsc2* inactivation relates more to a direct effect on tuberin rather than the interaction between the two proteins. However, more detailed *in vitro* studies will likely be necessary to define the specific molecular mechanisms involved.

While *Tsc1*^{GFAP1}CKO mice have been extensively characterized previously (18–25), care was taken in the current studies to ensure that similar experimental conditions were employed in replicating and directly comparing the phenotype of *Tsc1*^{GFAP1}CKO and *Tsc2*^{GFAP1}CKO mice. However, it is possible that other unforeseen differences between the *Tsc1*^{GFAP1}CKO and *Tsc2*^{GFAP1}CKO mice could have accounted for the observed differences between these lines. While both mouse colonies have been bred in the same SV129-C57Bl6 mixed genetic background, it is possible that slight differences in the relative contribution of the parental background strains could promote differences in the phenotypic features of the two colonies. However, SNP genotyping found no significant difference in the parental strain contribution between the two colonies, suggesting that the phenotypic differences between *Tsc1*^{GFAP1}CKO and *Tsc2*^{GFAP1}CKO mice were not caused by variability in the genetic background. Although laborious to complete, future studies involving breeding of both colonies into a pure genetic background should reduce any unanticipated effects of other genetic variability.

Independent of any differences between *Tsc1* and *Tsc2* gene inactivation, the creation of *Tsc2*^{GFAP1}CKO mice provides additional insights into the pathophysiology of neurological features of TSC. A number of different animal models have now been generated focusing on neurological aspects of TSC. Most of these models involve conditional *Tsc1* or *Tsc2* inactivation in different cell types by Cre-recombination driven by specific promoters, providing insights into the relative contribution of these cell types (neurons, glia, progenitor cells) at distinct stages of brain development (18,27,30,31). Although there are some differences between these models, particularly in the degree of glial versus neuronal abnormalities, there are also some overriding commonalities, such as progressive megencephaly and premature death. *Tsc2*^{GFAP1}CKO mice were created using a GFAP-Cre driver that leads predominantly to glial inactivation but also affects a subset of neurons, especially in hippocampus and cerebellum (32). While glial proliferation is very extensive and likely mediates many of the phenotypical abnormalities of *Tsc2*^{GFAP1}CKO mice, the relatively selective involvement of hippocampal neurons by Cre-mediated recombination of the *Tsc2* gene may account for the more extensive pathological abnormalities in hippocampus compared with neocortex, as well as contribute to the more severe epilepsy in these mice relative to *Tsc1*^{GFAP1}CKO mice. By comparison, a previous *Tsc2*^{GFAP2}CKO mouse was recently created, using a different GFAP-Cre line with earlier embryonic *Tsc2* inactivation of neuroglial progenitor cells compared with the present *Tsc2*^{GFAP1}CKO mice (27). As might be predicted, these previous *Tsc2*^{GFAP2}CKO appear to have an even more severe phenotype than either the *Tsc1*^{GFAP1}CKO or *Tsc2*^{GFAP1}CKO mice, with more diffuse neuronal involvement and even earlier mortality (27). Further refinements in mouse models of TSC, especially with regard to temporal and spatial specificity of *Tsc* gene inactivation, should continue to provide additional insights into the pathophysiology of TSC.

Finally, the effectiveness of rapamycin in preventing epilepsy and the corresponding histological abnormalities associated with epileptogenesis in *Tsc2*^{GFAP1}CKO mice not only provides evidence that the phenotypic differences between *Tsc1*^{GFAP1}CKO and *Tsc2*^{GFAP1}CKO mice are related to mTOR activation, but also has important clinical implications. Multiple studies have now demonstrated that mTOR inhibition is an effective treatment for epilepsy and other neurological deficits in TSC and related genetic animal models (26,31,33–35). While currently available seizure medications primarily suppress seizures symptomatically, the actions of rapamycin in this and some of the previous studies are consistent with an antiepileptogenic or disease-modifying effect in correcting underlying cellular mechanisms of epileptogenesis and preventing the progression of epilepsy. Future studies utilizing these and new animal models should provide further insights into mechanisms of epileptogenesis and lead to other, more effective therapeutic strategies for epilepsy in TSC.

MATERIALS AND METHODS

Animals and drug protocol

Care and use of animals were conducted according to an animal protocol approved by the Washington University Animal Studies Committee. *Tsc2*^{GFAP1}CKO mice were generated by a breeding strategy similar to that used to previously generate *Tsc1*^{GFAP1}CKO mice (18). *Tsc2*$^{flox/flox}$ mice (36) were first crossed with the same GFAP-Cre mouse line previously used to produce *Tsc1*^{GFAP1}CKO mice (18,29). Resulting *Tsc2*$^{flox/+}$;GFAP-Cre mice were then crossed with other *Tsc2*$^{flox/flox}$ mice to generate *Tsc2*$^{flox/flox}$;GFAP-Cre (*Tsc2*^{GFAP1}CKO) mice, as well as *Tsc2*$^{flow/flox}$;Wt and *Tsc2*$^{flox/+}$;GFAP-Cre mice. *Tsc2*$^{flow/flox}$ and *Tsc2*$^{flox/+}$;GFAP-Cre had no detectable phenotype and were used as controls for most experiments. For direct comparison, *Tsc1*^{GFAP1}CKO mice were again generated by a similar strategy as previously described (18). Based on the prior breeding of the respective founding colonies, both *Tsc1*^{GFAP1}CKO and *Tsc2*^{GFAP1}CKO mice have a similar mixed SV129/C57BL6 genetic background. To estimate the relative contribution of these parental background strains in each mouse colony, SNP analysis was performed by GenScreen (Harlan, Indianapolis, IN, USA), focusing on SNPs that are

known to be different between SV129 and C57BL6 mice. All groups were matched for sex and littermates.

Some *Tsc1*^{GFAP1}CKO and *Tsc2*^{GFAP1}CKO mice were monitored daily for survival with no interventions. In most studies, littermate control, *Tsc1*^{GFAP1}CKO and *Tsc2*^{GFAP1}CKO mice were used for western blot or histological studies or underwent video-EEG monitoring at pre-determined time points as described below. In one set of studies, rapamycin (3 mg/kg/day, 5 days/week) or vehicle treatment was initiated in *Tsc2*^{GFAP}CKO mice at postnatal day 14 and was continued until subsequent western blot, histological, video-EEG or survival analysis was completed at pre-determined time points. Rapamycin (LC Labs, Woburn, MA, USA) was initially dissolved in 100% ethanol, stored at −20°C and diluted in a vehicle solution containing 5% Tween 80, 5% PEG 400 (Sigma, St Louis, MO, USA) and 4% ethanol immediately before injection.

Western blot analysis

In 1-, 3- and 5-week-old mice, western blotting was performed to assay for the expression of phospho-S6, hamartin, tuberin and GLT-1 by standard methods (26). Briefly, neocortex and hippocampus were dissected and sonicated in Cell Lysis Buffer (Cell Signaling, Beverly, MA, USA). After centrifugation at 16,000 RPM for 1 h at 4°C, the supernatant was obtained and protein concentration was determined with the Bradford method (Pierce, Rockford, IL, USA). Equal amounts of total protein extract were separated by 10% SDS–PAGE and transferred to nitrocellulose membrane. After incubating with primary antibody to phospho-S6 (1:1000, Cell Signaling), S6 (1:1000, Cell Signaling), actin (1:5000, Sigma), GLT-1 (1:1000, Alpha Diagnostics, San Antonio, TX, USA), hamartin (1:1500, Cell Signaling), or tuberin (1:1500, Cell Signaling), the membranes were reacted with peroxidase-conjugated secondary antibody. Signals were detected by using enhanced chemiluminescence reagent (Pierce) and quantitatively analyzed with ImageJ software.

Histology/Immunohistochemistry

In 1-, 3-, 5- and 7-week-old mice, histological analysis was performed to assess glial proliferation and neuronal organization by standard methods (26). Briefly, mice were transcardially perfused with ice-cold phosphate buffered saline (PBS), pH 7.4, followed by 4% paraformaldehyde in PBS, pH 7.4. The brains were removed and post-fixed in 4% paraformaldehyde in PBS overnight at 4°C. Fixed brains were transferred to 30% sucrose for at least 24 h and then sectioned coronally with a vibratome at a thickness of 50 μm. For cresyl violet staining, sections were mounted and immersed in 0.5% cresyl violet for 5 min. For GFAP staining, sections were incubated with GFAP antibody (anti-rabbit, 1:500, Sigma) overnight at 4°C. After washing with PBS, the sections were incubated with Alexa 488-conjugated anti-rabbit IgG (1:500, Cell Signaling) and then cover-slipped with anti-fade mount solution (Molecular Probes). Images were acquired with a Zeiss LSM PASCAL confocal microscope. GFAP-immunoreactive cells in neocortex and hippocampus were counted by an investigator blinded to the treatment of the mice. In images from coronal sections at ∼2 mm posterior to bregma and ∼1 mm from midline, regions of interest were marked in neocortex by a 200 μm wide box spanning from the neocortical surface to the bottom of layer VI and in hippocampus by a 200 μm wide box spanning from the CA1 pyramidal cell layer to stratum lacunosum moleculare. GFAP-immunoreactive cells were quantified in the regions of interest from two sections per mouse from a total of six mice per group. For proliferating cell nuclear antigen (PCNA) assays, sections were stained for PCNA by the avidin–biotin peroxidase complex method according to kit instructions (Invitrogen, Camarillo, CA, USA). Sections were imaged by a Nanozoomer digital slide scanner (Olympus, Center Valley, PA, USA) and positive cells counted using similar methods as for GFAP quantification.

Video-EEG monitoring

Tsc1^{GFAP1}CKO and *Tsc2*^{GFAP1}CKO mice underwent weekly video-EEG monitoring starting at 3 weeks of age to assess seizure frequency, as described previously (23,26). In separate studies, vehicle-treated and rapamycin-treated *Tsc2*^{GFAP1}CKO mice also received video-EEG monitoring starting at 3 weeks. Briefly, four epidural screw electrodes were surgically implanted in mice under isoflurane anesthesia. Mice were allowed to recover from surgery for at least 24 h before recording. Continuous EEG data were saved digitally on personal computers using Grass P-100 AC amplifiers (Astro-Med, West Warwick, RI, USA), Axon Digidata A-D converters and Axoscope software (Molecular Devices, Sunnyvale, CA, USA). To determine the behavioral correlate of electrographic seizures, simultaneous digital video was recorded using a Sanyo Day-Night camera and a Darim MG-100 MPEG video capture card (Darim Vision Corp., Pleasanton, CA, USA). Forty-8 h epochs of continuous video-EEG data were obtained once a week from each mouse, until the animal died or the electrodes malfunctioned. Electrographic seizures were identified by their characteristic pattern of discrete periods of rhythmic spike discharges that evolved in frequency and amplitude lasting at least 10 s, typically ended with repetitive burst discharges, and followed by severe voltage suppression. On video analysis, the behavioral correlate to these seizures typically involved head bobbing, rearing with forelimb clonus and occasional generalized convulsive activity. Seizure frequencies (# seizures/48 h period) were calculated from each 48 h epoch.

Statistics

SigmaStat (Systat Software, San Jose, CA, USA) was used for statistical analysis. Quantitative differences between rapamycin or vehicle-treated *Tsc2*^{GFAP}CKO mice, *Tsc1*^{GFAP}CKO mice or littermate controls were analyzed by student's *t*-test when comparing two groups and by one-way ANOVA with Tukey multiple comparisons post-tests when comparing more than two groups. When data did not conform to a normal distribution, a non-parametric (Kruskal–Wallis) ANOVA was used. Quantitative data are expressed as mean ± standard error of the mean (SEM). Survival data

were analyzed by a Kaplan–Meier log-rank test. Statistical significance was defined as $P < 0.05$.

SUPPLEMENTARY MATERIAL

Supplementary Material is available at *HMG* online.

Conflicts of Interest statement. None declared.

FUNDING

This work was supported by the National Institutes of Health (K02NS045583 and R01NS056872 to M.W., P30 NS057105 to Washington University), the Tuberous Sclerosis Alliance (M.W.) and National Nature Science Foundation of China (81072621 to L.-H.Z.).

REFERENCES

1. Kwiatkowski, D.J. (2003) Tuberous sclerosis: from tubers to mTOR. *Ann. Hum. Genet.*, **67**, 87–96.
2. Crino, P.B., Nathanson, K.L. and Henske, E.P. (2006) The tuberous sclerosis complex. *N. Engl. J. Med.*, **355**, 1345–1356.
3. Holmes, G.L. and Stafstrom, C.E., and the Tuberous Sclerosis Study Group. (2007) Tuberous Sclerosis Complex and epilepsy: recent developments and future challenges. *Epilepsia*, **48**, 617–630.
4. Jones, A.C., Daniells, C.E., Snell, R.G., Tachataki, M., Idziaszczyk, S.A., Krawczak, M., Sampson, J.R. and Cheadle, J.P. (1997) Molecular genetic and phenotypic analysis reveals differences between TSC1 and TSC2 associated familial and sporadic tuberous sclerosis. *Hum. Mol. Genet.*, **6**, 2155–2161.
5. Dabora, S.L., Jozwiak, S., Franz, D.N., Roberts, P.S., Nieto, A., Chung, J., Coy, Y.S., Reeve, M.P., Thiele, E., Egelhoff, J.C. *et al.* (2001) Mutational analysis in a chort of 224 tuberous sclerosis patients indicates increased severity of TSC2, compared with TSC1, disease in multiple organs. *Am. J. Hum. Genet.*, **68**, 64–80.
6. Au, K.S., Williams, A.T., Roach, E.S., Batchelor, L., Sparagana, S.P., Delgado, M.R., Wheless, J.W., Baumgartner, J.E., Roa, B.B., Wilson, C.M. *et al.* (2007) Genotype/phenotype correlation in 325 individuals referred for a diagnosis of tuberous sclerosis complex in the United States. *Genet. Med.*, **9**, 88–100.
7. Jansen, F.E., Braams, O., Vincken, K.L., Algra, A., Anbeek, P., Jennekens-Schinkel, A., Halley, D., Zonnenberg, B.A., van den Ouweland, A., van Huffelen, A.C. *et al.* (2008) Overlapping neurologic and cognitive phenotypes in patients with TSC1 or TSC2 mutations. *Neurology*, **70**, 908–915.
8. Plank, T.L., Yeung, R.S. and Henske, E.P. (1998) Hamartin, the product of the tuberous sclerosis 1 (TSC1) gene, interacts with tuberin and appears to be localized to cytoplasmic vesicles. *Cancer Res.*, **58**, 4776–4770.
9. van Slegtenhorst, M., Nellist, M., Nagelkerken, B., Cheadle, J., Snell, R., van den Ouweland, A., Reuser, A., Sampson, J., Halley, D. and van der Sluijs, P. (1998) Interaction between hamartin and tuberin, the TSC1 and TSC2 gene products. *Hum. Mol. Genet.,* **7**, 1053–1057.
10. Gutmann, D.H., Zhang, Y., Hasbani, M.J., Goldberg, M.P., Plank, T.L. and Henske, E.P. (2000) Expression of the tuberous sclerosis complex (TSC) gene products, hamartin and tuberin, in central nervous system tissues. *Acta Neuropathol.*, **99**, 223–230.
11. Inoki, K., Li, Y., Xu, T. and Guan, K.L. (2003) Rheb GTPase is a direct target of TSC2 GAP activity and regulates mTOR signaling. *Genes Dev.*, **17**, 1829–1834.
12. Zhang, Y., Gao, X., Saucedo, L.J., Ru, B., Edgar, B.A. and Pan, D. (2003) Rheb is a direct target of the tuberous sclerosis tumor suppressor proteins. *Nat. Cell Biol.*, **5**, 578–581.
13. Gao, X., Zhang, Y., Arrazola, P., Hino, O., Kobayashi, T., Yeung, R.S., Ru, B. and Pan, D. (2002) Tsc tumour suppressor proteins antagonize amino acid-TOR signalling. *Nat. Cell Biol.*, **4**, 699–704.
14. Inoki, K., Li, Y., Zhu, T., Wu, J. and Guan, K.L. (2002) TSC2 is phosphorylated and inhibited by Akt and suppresses mTOR signaling. *Nat. Cell Biol.*, **4**, 648–657.
15. Tee, A.R., Fingar, D.C., Manning, B.D., Kwaitkowski, D.J., Cantley, L.C. and Blenis, J. (2002) Tuberous sclerosis complex-1 and -2 gene products function together to inhibit mammalian target of rapamycin (mTOR)-mediated downstream signaling. *Proc. Natl Acad. Sci. USA*, **99**, 13571–13576.
16. El-Hashemite, N., Zhang, H., Henske, E.P. and Kwiatkowski, D.J. (2003) Mutation in TSC2 and activation of mammalian target of rapamycin signaling pathway in renal angiomyolipoma. *Lancet*, **361**, 1348–1349.
17. Maheshwar, M.M., Cheadle, J.P. and Jones, A.C. (1997) The GAP-related domain of tuberin, the product of the *TSC*2 gene, is a target for missense mutations in tuberous sclerosis. *Hum. Mol. Genet.*, **6**, 1991–1996.
18. Uhlmann, E.J., Wong, M., Baldwin, R.L., Bajenaru, M.L., Onda, H., Kwiatkowski, D.J., Yamada, K.A. and Gutmann, D.H. (2002) Astrocyte-specific TSC1 conditional knockout mice exhibit abnormal neuronal organization and seizures. *Ann. Neurol.*, **52**, 285–296.
19. Wong, M., Ess, K.E., Uhlmann, E.J., Jansen, L.A., Li, W., Crino, P.B., Mennerick, S., Yamada, K.A. and Gutmann, D.H. (2003) Impaired astrocyte glutamate transport in a mouse epilepsy model of tuberous sclerosis complex. *Ann. Neurol.*, **54**, 251–256.
20. Uhlmann, E.J., Li, W., Scheidenhelm, D.K., Gau, C.L., Tamanoi, F. and Gutmann, D.H. (2004) Loss of tuberous sclerosis complex 1 (Tsc1) expression results in increased Rheb/S6K pathway signaling important for astrocyte cell size regulation. *Glia*, **47**, 180–188.
21. Ess, K.C., Uhlmann, E.J., Li, W., Li, H., DeClue, J.E., Crino, P.B. and Gutmann, D.H. (2004) Expression profiling in tuberous sclerosis complex (TSC) knockout mouse astrocytes to characterize human TSC brain pathology. *Glia*, **46**, 28–40.
22. Jansen, L.A., Uhlmann, E.J., Crino, P.B., Gutmann, D.H. and Wong, M. (2005) Epileptogenesis and reduced inward rectifier potassium current in *Tuberous Sclerosis Complex-1* deficient astrocytes. *Epilepsia*, **46**, 1871–1880.
23. Erbayat-Altay, E., Zeng, L.H., Xu, L., Gutmann, D and Wong, M. (2007) The natural history and treatment of epilepsy in a murine model of tuberous sclerosis. *Epilepsia*, **48**, 1470–1476.
24. Zeng, L.H., Ouyang, Y., Gazit, V., Cirrito, J.R., Jansen, L.A., Ess, K.C, Yamada, K.A., Wozniak, D.F., Holtzman, D.M., Gutmann, D.H and Wong, M. (2007) Abnormal glutamate homeostasis and impaired synaptic plasticity and learning in a mouse model of tuberous sclerosis complex. *Neurobiol. Dis.*, **28**, 184–196.
25. Xu, L., Zeng, L.H. and Wong, M. (2009) Impaired astrocyte gap junction coupling and potassium buffering in a mouse model of Tuberous Sclerosis Complex. *Neurobiol. Dis.*, **34**, 291–299.
26. Zeng, L.H., Xu, L., Gutmann, D.H. and Wong, M. (2008) Rapamycin prevents epilepsy in a mouse model of tuberous sclerosis complex. *Ann. Neurol.*, **63**, 444–453.
27. Way, S.W., McKenna, J. 3rd, Mietzsch, U., Reith, R.M, Wu, H.C and Gambello, M.J. (2009) Loss of Tsc2 in radial glia models the brain pathology of tuberous sclerosis complex in the mouse. *Hum. Mol. Genet.*, **18**, 1252–1265.
28. Zhou, L., Theis, M., Alvarez-Maya, I., Brenner, M., Willecke, K and Messing, A. (2001) hGFAP-cre transgenic mice for manipulation of glial and neuronal function *in vivo*. *Genesis*, **31**, 85–94.
29. Bajenaru, M.L., Zhu, Y., Hedrick, N.M., Donahoe, J., Parada, L.F. and Gutmann, D.H. (2002) Astrocyte-specific inactivation of the neurofibromatosis (NF1) gene is insufficient for astrocytoma formation. *Mol. Cell. Biol.*, **22**, 5100–5113.
30. Meikle, L., Talos, D.M., Onda, H., Pollizzi, K., Rotenberg, A., Sahin, M., Jensen, F.E. and Kwiatkowski, D.J. (2007) A mouse model of tuberous sclerosis: neuronal loss of Tsc1 causes dysplastic and ectopic neurons, reduced myelination, seizure activity, and limited survival. *J. Neurosci.,* **27**, 5546–5558.
31. Zhou, J., Blundell, J., Ogawa, S., Kwon, C.H., Zhang, W., Sinton, C., Powell, C.M. and Parada, L.F. (2009) Pharmacological inhibition of mTORC1 suppresses anatomical, cellular, and behavioral abnormalities in neural-specific Pten knock-out mice. *J. Neurosci.*, **29**, 1773–1783.
32. Fraser, M.M., Zhu, X., Kwon, C.H., Uhlmann, E.J., Gutmann, D.H. and Baker, S.J. (2004) Pten loss causes hypertrophy and increased proliferation of astrocytes *in vivo*. *Cancer Res.*, **64**, 7773–7779.
33. Meikle, L., Pollizzi, K., Egnor, A., Kramvis, I., Lane, H., Sahin, M. and Kwiatkowski, D.J. (2008) Response of a neuronal model of

tuberous sclerosis to mammalian target of rapamycin (mTOR) inhibitors: effects on mTORC1 and Akt signaling lead to improved survival and function. *J. Neurosci.,* **28**, 5422–5432.
34. Ehninger, D., Han, S., Shilyansky, C., Zhou, Y., Li, W., Kwiatkowski, D.J., Ramesh, V. and Silva, A.J. (2008) Reversal of learning deficits in a Tsc2(+/−) mouse model of tuberous sclerosis. *Nat. Med.,* **14**, 843–848.
35. Ljungberg, M.C., Sunnen, C.N., Lugo, J.N., Anderson, A.E. and D'Arcangelo, G. (2009) Rapamycin suppresses seizures and neuronal hypertrophy in a mouse model of cortical dysplasia. *Dis. Model Mech.,* **2**, 389–398.
36. Hernandez, O., Way, S., McKenna, J. III and Gambello, M.J. (2007) Generation of a conditional disruption of the Tsc2 gene. *Genesis,* **45**, 101–106.